Engine Thermal Efficiency Gain and Well-to-Wheel Greenhouse Gas Savings When Using Bioethanol as a Gasoline-Blending Component in Future Spark-Ignition Engines: A China Case Study

Wang, C., Herreros, J. M., Jiang, C., Sahu, A. & Xu, H.

Original citation & hyperlink:
Wang, C, Herreros, JM, Jiang, C, Sahu, A & Xu, H 2018, 'Engine Thermal Efficiency Gain and Well-to-Wheel Greenhouse Gas Savings When Using Bioethanol as a Gasoline-Blending Component in Future Spark-Ignition Engines: A China Case Study' Energy & Fuels, vol. 32, no. 2, pp. 1724-1732.
https://dx.doi.org/10.1021/acs.energyfuels.7b02110

DOI 10.1021/acs.energyfuels.7b02110
ISSN 0887-0624
ESSN 1520-5029

Publisher: American Chemical Society

Engine Thermal Efficiency Gain and WTW GHG Savings when using Bioethanol as a Gasoline-Blending Component in Future SI engine: A China Case Study

Chongming Wang[1,2], Jose Martin Herreros[1], Amrit Sahu[1], Changzhao Jiang[3], Hongming Xu[1]

[1] University of Birmingham, Department of Mechanical Engineering, Birmingham, UK, B15 2TT

[2] Coventry University, School of Engineering, Coventry, UK, CV1 5FB

[3] Loughborough University, Aeronautical and Automotive Engineering, Leicestershire, UK, LE11 3TU

Abstract: In 2017, the Chinese government has issued a strategic policy of nationwide use of bioethanol as a gasoline-blending component by 2020 for the considerations of reducing smog and greenhouse gas (GHG) emissions; therefore, it is highly relevant to estimate the benefits of well-to-wheel (WTW) GHG emission savings using future engine technologies. However, literature about the WTW GHG emissions for ethanol blends did not cover the engine efficiency gains in engines with future technologies. In a previous publication from authors' group, an empirical model was developed to predict the anti-knock property and engine thermal efficiency gains of ethanol blends in spark-ignition (SI) engines. This paper is a follow-up study, not only looking at the potential engine thermal efficiency gains, also WTW GHG emissions in future engine technology. More specifically, a case study of adding bioethanol into two representative E10 fuels (main- and premium-octane grade fuel) from China was conducted. It is assumed that the future engine technology enables adjustable compression ratio (CR) according to the octane rating of ethanol blends, allowing the maximum extraction of the benefit of high anti-knock property of ethanol blends. In addition, the sensitivity of GHG intensity of bioethanol on WTW GHG emissions is analysed and discussed. It is found that the chemical and cooling effects of ethanol blends are the dominant factors contributing to engine thermal efficiency gains. For the ethanol blends with the RON84.5 base gasoline, the negative impact of lower heating value (LHV) of ethanol blends on the vehicle mileage range can be completely offset by the engine thermal efficiency gain enabled by higher octane rating of ethanol blends. Assuming that in China in the future bioethanol has a GHG intensity of 33 gCO_2-eq/MJ (gram of CO_2 equivalent per megajoules of lower heating value), compared to E10, E30 led to a 21.2% reduction of WTW GHG emissions in a turbocharged (TC) direct-injection spark-ignition (DISI) vehicle. Among this 21.2% reduction, one third is due to the thermal efficiency gain and two third is due to the use of renewable bioethanol. Reducing the GHG intensity of bioethanol is a key to reducing WTW GHG emissions. For the TC DISI engine technology, when E20 is used instead of E10, every 1 gCO_2-eq/MJ reduction in GHG intensity of bioethanol leads to 0.441 gCO_2-eq/MJ of WTW GHG emissions.

Keywords: Bioethanol; Thermal Efficiency; WTW; GHG

ACRONYMS AND ABBREVIATIONS

CFR	Cooperative Fuel Research	**PCCE**	Partially Captured Cooling Effect
CR	Compression Ratio	**PRFs**	Primary Reference Fuels
DISI	Direct Injection Spark Ignition	**RON**	Research Octane Number
EOI	Effective Octane Index	**RON_{blend}**	RON of Ethanol Blend
GHG	Greenhouse Gas	**RON_{base}**	RON of Base Gasoline
LHV	Lower Heating Value	**$RON_{ethanol}$**	RON of Ethanol
MON	Motor Octane Number	**SI**	Spark-ignition
NA	Naturally Aspirated	**TC**	Turbo-Charged
ONCE	Octane Number from Cooling Effect	**WTT**	Well-to-tank
$ONCE_{gasoline}$	ONCE of Base Gasoline	**WTW**	Well-to-wheel
$ONCE_{ethanol}$	ONCE of Ethanol		

DEFINITIONS

E'x'	x vol.% ethanol in the blend
K	A scaling factor used in the calculation of Octane Index
S	Octane sensitivity (RON and MON)
x_{vol}	vol.% of ethanol in the blend

Octane related parameter:

EOI = chemical effect + octane sensitivity effect + cooling effect

Chemical effect = RON-PCCE

Octane sensitivity effect = -K*S

Cooling effect = ONCE

1 Introduction

Progressive research on biofuels has been conducted for improving the sustainability of energy supplies and reducing greenhouse gas (GHG) emissions[1]. Among the biofuel candidates for spark-ignition (SI) engines, bioethanol is the most widely. Studies have proven ethanol/blends in improving engine efficiency, in reducing emissions, such as particulates and unburned hydrocarbons[2-5], and in reducing deposit formation[6].

Table 1 lists a summary of gasoline and ethanol properties. The high octane rating of ethanol reduces engine knock tendency, thus high compression ratio (CR) can be used, leading to higher thermal efficiency[7]. Recent studies have shown that the high octane sensitivity of ethanol also contributes to suppressing knock in SI engines[8-11].

Table 1: Fuel properties

	Unit	Gasoline*	Ethanol
Formula		C_4-C_{12}	C_2H_6O
RON		89+	107
MON		79+	89
Oxygen content	*wt*.%	0	34.78
Stoichiometric air-fuel ratio		14.5	9
Density @ 15ºC	kg/m^3	720-775	790
Lower heating value	MJ/kg	42	26.9
Flashpoint	°C	-40	13
Heat of vaporization @ λ=1	kJ/kg_air	26	103
Initial boiling point	°C	varies	78
Reid vapour pressure	kPa	Varies (48-110)	15.5
Water solubility	%	0	100

* Typical gasoline available in the China market.

There are two types of blending techniques for the use of bioethanol as a gasoline blending component: splash blending and RON-match blending techniques. Splash blending refers to a process that ethanol is directly added to a base gasoline, leading to a final fuel with a higher RON rating. RON-match blending refers to a process that ethanol is added to a base gasoline whose RON rating is adjusted according to the ethanol content, leading to a final fuel with a pre-determined RON rating. A blend with a higher ethanol content means that the requirement of RON for the base gasoline is lower. The RON-match blended ethanol fuels lead to a limited fuel efficiency gain. In the following paper, only splash blended ethanol are discussed.

In 2016, China only used three million tonnes of renewable fuels, less than one percent of total fuel consumption and approximately 2% of total gasoline consumption[12]. In 2017, for the considerations of reducing smog and GHG emissions, the Chinese government has issued a strategic policy of nationwide use of bioethanol as a gasoline blending component by 2020. China is the world's third-largest ethanol producer (2.1 million tonnes/year) behind Brazil and the United States. Currently, most of the bioethanol (64%) is produced from corn, followed by wheat and cassava; however, by 2025 Chinese government aims to promote the large-scale domestic production of the second generation cellulosic bioethanol made from feedstocks such as grasses and crop waste.

There is literature available for the life cycle analysis (LCA) of bioethanol produced in China[13-17]. Zhang et al.[13] investigated cassava-based bioethanols in China and concluded that the net energy and GHG emissions of cassava-based bioethanol were approximately 13.64 MJ/L and 1473 gCO_2-eq/L, respectively. Ethanol conversion process accounts for the most energy consumption and GHG emissions. The water footprint of cassava-based ethanol was approximately 2998 m^3/tonne, among which the cassava-planting is the most water-intensive due to the grey-water from the use of fertilizer.

Yand and Chen[18] studied GHG emissions of corn-based bioethanol in China, and they found that GHG intensity for corn-based ethanol can be as high as of 11610 gCO_2-eq/kg_ethanol; however, They also pointed out that corn-based bioethanol might lead to a 98% GHG reduction compared to gasoline when an ecological system with production chain featuring constructed wetland, biogas and combined heat and power are fully employed.

Ren et al.[14] examined bioethanols produced from various feedstocks in China using a tool called Data Envelopment Analysis (DEA). The feedstock included wheat, corn, cassava and sweet potatoes, The status of each feedstock was classified as 'old', 'new', 'wet' and 'dry'. They found that only wheat-based and sweet-potato-based bioethanols were energy-efficient in China.

Zhao et al.[15] conducted LCA of corn-stover-based bioethanol in China, based on several scenarios using current and future technology for ethanol conversion process. They found that the GHG intensity of corn-stover-based bioethanol was approximately 40 gCO_2-eq/MJ. Compared to gasoline, the WTW GHG emission reduction of corn-stover-based bioethanol was 52%-55%, and the savings of fossil fuel were approximately 72%-76%. GHG emissions from the ethanol conversion process and combustion process accounted for 51%-55%, and 36%-37% of the total lifecycle GHG emissions. Zhao et al. pointed out that the data presented in the study was sensitive to allocation methods used in LCA.

The literature[13-17] agrees that the LCA GHG results are highly dependent on methods and data such as bioethanol yield rate, energy inputs. Therefore, the results have large uncertainties. On the other hand, the above literature mainly focuses on the feedstock planting and bioethanol conversion processes; whilst the engine efficiency gains of bioethanol blends in future engine technology are not studied. It is important to estimate the engine thermal efficiency gain and the GHG emission savings when using bioethanol blends in future engines. Engine testing at specific operating conditions does not reveal generic benefits of ethanol blends because data can only be applied to a specific engine hardware design or operating conditions/testing cycles. On the other hand, most current engines do not fully make use of the high octane of ethanol blends, because only active ignition management system is used. If engine CR is adjustable to suit the high octane of ethanol blends, more benefits would be extracted.

In the previous publication[19] from authors' group, a model was developed to predict RON, cooling effect and CR gain using ethanol blends. The model assumes that the engine CR is adjustable for the purpose of maximising the advantage of high octane rating of ethanol blends. In this paper, this model is used for a case study of adding bioethanol into two representative base gasoline in China (main- and premium-octane grade), with the focuses on the engine thermal efficiency gain and well to wheel (WTW) GHG savings.

The novelty of this paper is that it uses an empirical model to estimate the engine thermal efficiency gains of ethanol-gasoline blends under future engine technology. In addition, using GHG emission data of bioethanol and gasoline in China from the literature, and the aforementioned engine thermal efficiency gains, this paper presents the estimated WTW GHG savings.

In the following section, a brief overview of the empirical model will be presented, followed by a discussion of engine thermal efficiency gains and GHG savings from ethanol blends using two Chinese gasoline as base fuels. In the end, limitation of this work is presented.

2 Brief Overview of Ethanol Blends Model

Figure 1 briefly described the empirical model for SI engines fuelled with ethanol blends, capable of predicting RON, octane sensitivity, cooling effect, and engine thermal efficiency improvement[19]. An effective octane index (EOI), which considers RON, octane sensitivity and cooling effect (heat of vaporisation), is used to determine ethanol blends' anti-knock properties. Additionally, the high flame speed and engine downsizing also improve engine thermal efficiency. It should be noted that the empirical model only works for ethanol blends with up to 70 vol.%.

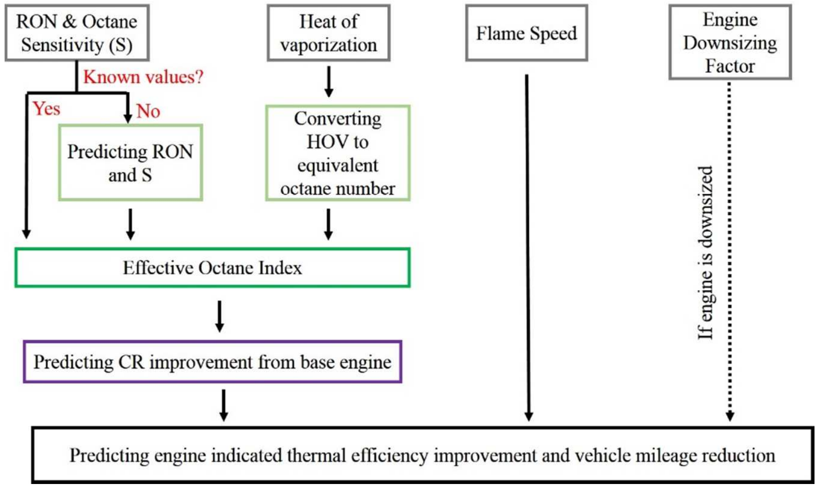

Figure 1: Empirical model for SI engines using ethanol blends

RON of ethanol blend is calculated via:

$$\text{Equation 1:} \quad \mathrm{RON_{blend}} = \frac{(-0.01983 x_{vol}{}^2 + 2.8512 x_{vol}) \times (\mathrm{RON_{ethanol}} - \mathrm{RON_{base}})}{100} + \mathrm{RON_{base}}$$

where $\mathrm{RON_{blend}}$, $\mathrm{RON_{ethanol}}$ and $\mathrm{RON_{base}}$ are the RON of ethanol blend, ethanol and base gasoline, respectively; x_{vol} is the volumetric content of ethanol.

In direct-injection spark-ignition (DISI) engines, apart from the fuel's octane rating, the charge cooling effect (heat of vaporisation) of the fuel is another important contributor in suppressing knock. The charge cooling effect is quantitatively converted into equivalent octane number. ONCE is abbreviated from octane number from the cooling effect. ∆ONCE between ethanol blends and base gasoline can be expressed by the following equation[19]:

$$\text{Equation 2:} \quad \Delta\,\mathrm{ONCE} = \mathrm{ONCE_{blend}} - \mathrm{ONCE_{base}} = 0.1543 \times \mathrm{x_{vol}}$$

The charge cooling effect is partially captured in the RON test in cooperative fuels research (CFR) engine. The partially captured cooling effect (PCCE) in the standard RON test is quantified as:

$$\text{Equation 3:} \quad \mathrm{PCCE} = 0.00028 \times x_{vol}{}^2 + 0.0200 \times \mathrm{x_{vol}}$$

In order to reflect octane effect, cooling effect and octane sensitivity effect of ethanol in modern DISI engines, EOI is used to describe ethanol's anti-knock property[19]:

$$\text{Equation 4:} \quad \mathrm{EOI} = (\mathrm{RON} - \mathrm{K} \times \mathrm{S}) + (\mathrm{ONCE} - \mathrm{PCCE}) = (\mathrm{RON} - \mathrm{PCCE}) - \mathrm{K} \times \mathrm{S} + \mathrm{ONCE}$$

where K is a scaling factor depending solely on the in-cylinder temperature and pressure history experienced by the end-gas prior to the onset of auto-ignition. The typical octane sensitivity (S=RON-MON) for gasoline is 10. The octane sensitivity for ethanol is 18. The octane sensitivity of ethanol blends can be linearly estimated from the octane sensitivity of gasoline and ethanol[19]. Thus, EOI considers: (1) chemical effect (RON-PCCE); (2) octane sensitivity effect (-K*S); (3) cooling effect (ONCE). An engine survey revealed that the average K values across a wide range of engine operating conditions were 0 and -0.3 for current natural aspirated (NA) SI engines and current turbocharged (TC) DISI engines, respectively[20].

Ref.[11] suggested that every 4 unit octane increase allows 1 unit increase of CR (ΔEOI/ΔCR=4). Ref[21] suggested ΔEOI/ΔCR=3. In authors' review paper[19], after collecting data from more than ten publications, it recommended ΔEOI/ΔCR=4. More detailed experimental data regarding CR and octane number are available in Ref.[19] In this paper, in order to reflect different engine types and technologies, ΔEOI/ΔCR=3~4 is used.

The marginal benefit of CR on engine thermal efficiency (η) gain reduces with the increasing of CR. However, as presented in authors' review paper[19], for CR in the range of 8:1-14:1, the thermal efficiency gain with CR is almost linear ($\Delta\eta$/ΔCR=1.8%). The contribution of the high flame speed of ethanol to thermal efficiency is $\Delta\eta$=0.20% for every 10 vol.% ethanol content in blends[19]. Engine downsizing is a technology that increases engine thermal efficiency by allowing an engine to operate at more efficient high load regimes, instead of at low load regimes where pumping losses significantly reduce engine thermal efficiencies. In Ref.[21], it is suggested that the thermal efficiency increase multiplier from additional engine downsizing for TC DISI engines is 1.1. More detail of this empirical model is available in Ref.[19].

3 Results and discussion

This section contains two parts. In part one, the engine thermal efficiency gain is modelled for various ethanol blends. The CR of engines is generally not adjustable, however, in this study, it is assumed that the future engine technology allows adjustable CR to match the octane rating of the fuel. In part two, the WTW GHG emission savings from ethanol blends are investigated, along with the discussion of the sensitivity of GHG intensity bioethanol.

3.1 Engine Thermal Efficiency

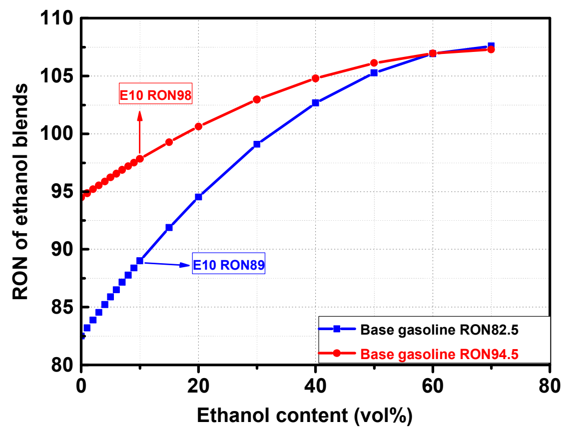

Figure 2: RON of ethanol blends using two base gasoline fuels

RON of ethanol blends: Figure 2 shows the RON of ethanol blends using two base gasoline fuels, RON82.5 and RON94.5. Adding 10 vol.% ethanol into these two base gasoline fuels produces E10 with RON of 89 and 98, respectively, representing the regular- and premium-octane grade gasoline in the China Market. From Figure 2, it can be seen that: (1) RON of ethanol blends increases with ethanol content; however, the margin reduces especially at medium and high ethanol content; (2) at the same ethanol content, RON gain is higher for the low RON base gasoline (RON84.5) than the high RON base gasoline (RON94.5). The RON gap of ethanol blends with the low- and high-RON gasoline base fuels narrowed from 12 at E0 to 5 at E40. In Figure 2, there is limited RON improvement when ethanol content is increased from 40 vol.% to 70 vol.%. As an octane improver, ethanol shows the best octane boosting effect at low blend ratios and in the low octane rating base gasoline.

Thermal Efficiency Gain: Figure 3 shows engine thermal efficiency gain for ethanol blends in TC

DISI engines (K=-0.3). As mentioned earlier in this paper, in order to reflect different engine types and technologies, ΔEOI/ΔCR varies between 3 to 4. For engines with better combustion system designs, engines have less knocking tendency; therefore, ΔEOI/ΔCR=3; otherwise ΔEOI/ΔCR=4. This assumption introduces some uncertainties to potential engine thermal efficiency gain; therefore, the results can be applied broadly. From Figure 3, it can be seen that ethanol blends using RON82.5 base gasoline lead to more engine thermal efficiency gain than that using RON94.5 base gasoline.

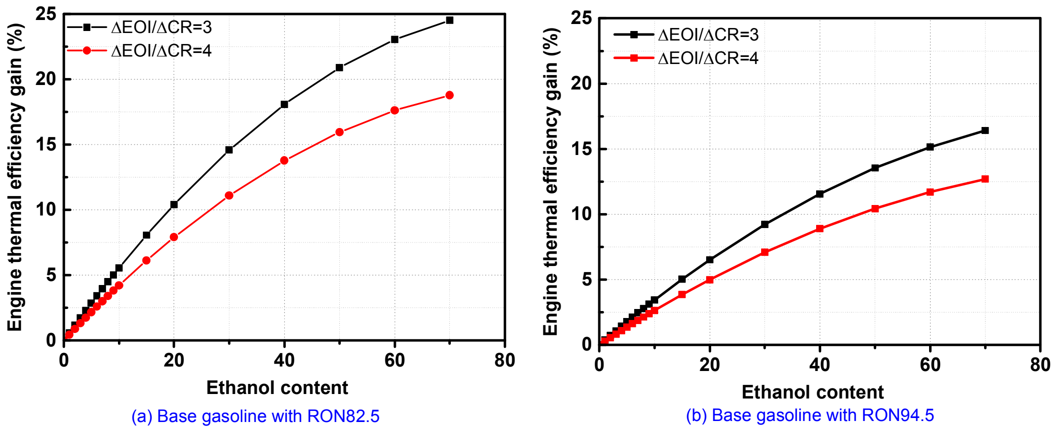

Figure 3: Engine thermal efficiency gain for ethanol blends in TC DISI engines: (a) base gasoline with RON82.5; (b) base gasoline with RON94.5 (K=-0.3)

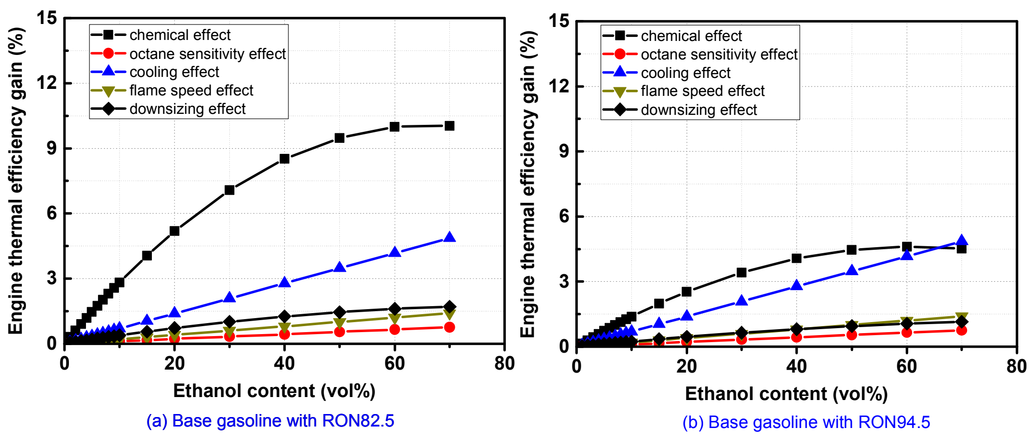

Figure 4: Breakdown of thermal efficiency gains for ethanol blends in TC DISI engines: (a) base gasoline with RON82.5; (b) base gasoline with RON94.5 (ΔEOI/ΔCR=4)

Figure 4 shows break down thermal efficiency gains for ethanol blends in TC DISI engines. Figure 4 only presented the results of ΔEOI/ΔCR=4. As mentioned earlier, EOI = chemical effect + octane sensitivity effect + cooling effect, where the chemical effect equals to RON-PCCE; the octane sensitivity effect equals to -K*S; the cooling effect equals to ONCE. In the TC DISI engine, the average K is -0.3; therefore, octane sensitivity effect is -0.3*S[20]. It should be pointed out that K values vary in the engine-operating map, and it only matters when the engine is operated at the knock-limited region of the engine map. The use of an average K value would underestimate the benefit of octane sensitivity at knock-limited engine load; whilst it would overestimate the benefit at knock-free engine load.

For the TC DISI engine fuelled with ethanol blends using RON82.5 base gasoline, the ranking contributing factor is chemical effect > cooling effect > downsizing effect > flame speed effect > octane sensitivity effect. For the TC DISI engine fuelled with ethanol blends using RON94.5 base gasoline, the ranking contributing factor is chemical effect > cooling effect > downsizing effect ≈ flame speed effect > octane sensitivity effect. The contribution of the chemical effect of the engine thermal efficiency gain reduces with the ethanol content. Overall, the chemical and cooling effects are the dominant factors contributing to engine thermal efficiency gain.

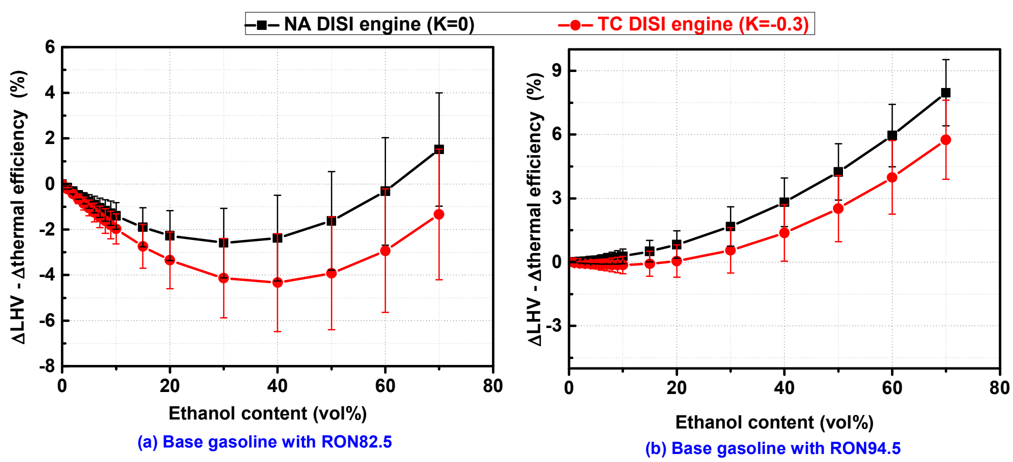

Figure 5: LHV reduction minus thermal efficiency gain for ethanol blends in NA DISI and TC DISI engines: (a) base gasoline with RON82.5; (b) base gasoline with RON94.5

LHV reduction: Figure 5 shows the LHV reduction minus thermal efficiency gain for ethanol blends in NA DISI (K=0) and TC DISI (K=-3) engines using two base gasoline fuels, RON82.5 and RON94.5. The error bars reflect ΔEOI/ΔCR=3~4, and the solid points in Figure 5 represent the results for ΔEOI/ΔCR=3.5. Assuming that the fuel tank size is fixed, the vehicle mileage range reduction can be estimated by subtracting LHV reduction by the engine thermal efficiency gain. For the ethanol blends with the high RON base fuel, it can be seen that it is possible to use high ethanol blends without significantly deteriorating the vehicle mileage range (Figure 5(a)). For the ethanol blends with the high RON base fuel, it is difficult to make up the LHV difference for higher ethanol blends via engine efficiency gains (Figure 5(b)). It has to be pointed out that the LHVs of the two base gasoline fuels are assumed to be 42 MJ/kg, a typical value for gasoline fuels. If the LHV of base gasoline is higher than 42 MJ/kg, the reduction of LHV for ethanol blends presented in Figure 5 would be underestimated, and vice versa. The above analysis is based on the assumption that the fuel tank size is fixed; however, the fuel tank size can be adjusted according to ethanol blends.

3.2 Vehicle WTW GHG Emission Analysis

In this section, in order to conduct an analysis of vehicle WTW GHG emissions, vehicle energy/fuel consumption data is required. In Ref.[22], a fuel consumption survey was conducted for 2555 vehicle models. It revealed that fuel consumption correlates well with the vehicle mass. When using main-grade gasoline in China (E10 with the RON 84.5 base gasoline), for a vehicle with a mass in the range of 1000-1500 kg and 1500-2000 kg, the average fuel consumptions are approximately 6.9 and 9.0 L/100km, respectively. Therefore, these two average fuel consumptions are used as for scenario studies for the Vehicle A (6.9 L/km) and Vehicle B (9.0 L/km). Based on the fuel consumption, energy consumption per kilometre can be estimated from lower heating values of base gasoline and ethanol. In this part, the engine thermal efficiency gain is estimated to be the same as the reduction of vehicle fuel consumption.

The CR of the engine of this vehicle is assumed to be adaptable for ethanol blends. Consequently, the engine thermal efficiency is improved, so as the fuel consumption and the WTW GHG emissions. In addition to engine thermal efficiency gain, the renewable bioethanol in the blend also contributes to the reduction of the WTW GHG emissions. The GHG intensity of ethanol needs to be defined. The ethanol GHG intensity varies, depending on the raw stock and the energy used to produce ethanol[23]. Currently, most of the bioethanol (64%) is produced from corn, followed by wheat and cassava. Zhang et al.[13] investigated cassava-based bioethanols produced in China and they concluded that the GHG intensity of cassava-based ethanol is approximately 1473 gCO_2-eq/L, which corresponding to 69.3 gCO2-eq/MJ. Zhao et al.[15] conducted LCA of corn-stover-based bioethanol in China. They found that the GHG intensity of corn-stover-based bioethanol is approximately 40 gCO2-eq/MJ. Therefore, the GHG intensity of corn-stover-based bioethanol is about 75% lower than that of cassava-based ethanol. By 2025 Chinese government aims to promote the large-scale domestic production of second generation cellulosic biofuels made from sources such as grasses, trees and crop waste. Therefore, it is necessary for study the sensitivity of GHG intensity of bioethanol on WTW GHG emissions. Table 2 listed the GHG intensities of various types of bioethanol. Overall, the 2G bioethanol has lower GHG intensity than the 1G bioethanol. In the following section, in order to reflect the GHG intensity of bioethanol in future in China, the GHG intensity of 33 gCO_2-eq /MJ, corresponding to the value of sugar-beet-based bioethanol in Table 2, is used. The sensitivity of GHG intensity of bioethanol on WTW GHG emissions is also analysed and discussed.

Table 2: GHG (CO_2 equivalent) intensity of various ethanol (Data from Ref[23])

	Ethanol type	GHG Intensity (gCO_2-eq/MJ)
1G ethanol	sugar beet ethanol	33
	wheat ethanol (natural gas as process fuel in a conventional boiler	46
	wheat ethanol (straw as process fuel in combined heat & power plant)	39
	wheat ethanol (natural gas as process fuel in combined heat & power plant)	26
	corn ethanol (natural gas as process fuel in combined heat & power plant)	37
	Sugarcane ethanol	24
2G ethanol	wheat straw ethanol	11
	waste wood ethanol	17
	farmed wood ethanol	20

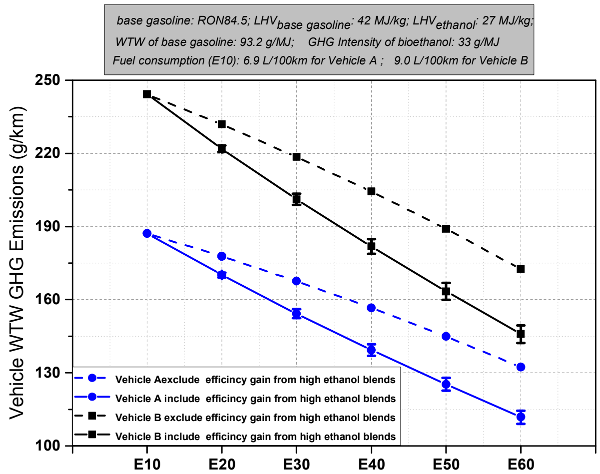

Figure 6: WTW GHG emissions (CO_2 equivalent) for ethanol blends in a TC DISI passenger vehicle

Figure 6 shows the WTW GHG emissions (CO_2 equivalent) of ethanol blends. As mentioned earlier, two vehicles, Vehicle A and Vehicle B, with fuel consumption of 6.9 and 9.0 L/km, respectively, were analysed. The ethanol GHG intensity is assumed to be 33 gCO_2-eq/MJ[23]. The WTW GHG emission of gasoline produced in China is typically in the range of 92-99 gCO_2-eq/MJ, depending on the fossil oil sources, refinery technologies and gasoline quality[15, 24]. In this study, the value of 93.2 gCO_2-eq/MJ for the base gasoline is used. Based on the fuel consumption, energy consumption per kilometre can be estimated from lower heating values of base gasoline and ethanol; therefore, Vehicle A and Vehicle B have 187 and 244 g/km GHG emissions for E10, respectively. In Figure 6, the GHG emissions savings with/without engine thermal efficiency gains are presented for both Vehicle A and Vehicle B. From Figure 6, it can be seen that: (1) vehicle B with a higher fuel consumption leads to higher marginal GHG emission reduction when ethanol is added to the blend in compared with Vehicle A with a lower fuel consumption; (2) The reduction is linear to ethanol content.

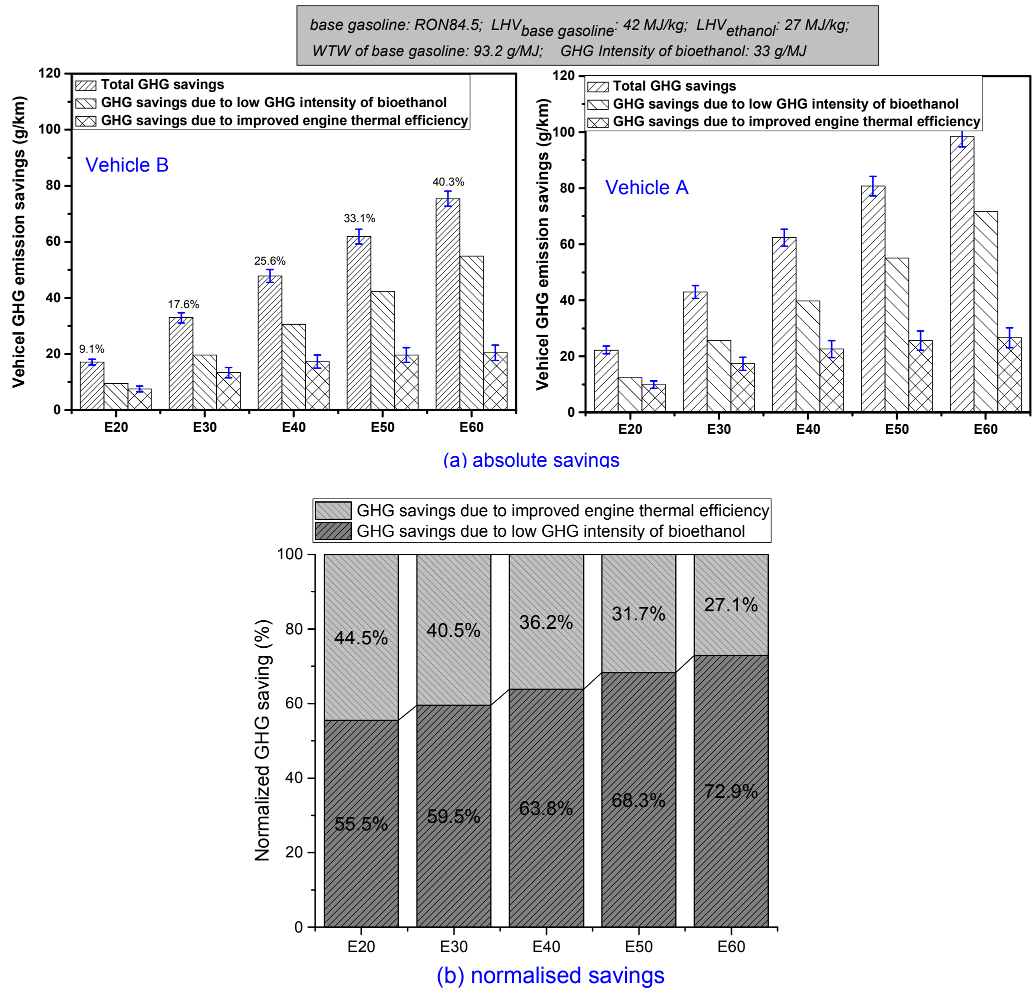

Figure 7: Breakdown of WTW GHG savings with E10 as the reference case in a TC DISI passenger vehicle (a) absolute savings; (b) normalised savings

Figure 7 shows the breakdown of WTW GHG savings compared to the E10 case for ethanol blends in the TC DISI passenger vehicle. The number above the column in Figure 7 (a) shows the total savings in comparison to E10. The total savings increases almost linearly with ethanol content, due to the low GHG intensity of bioethanol and improved engine thermal efficiency. The marginal GHG saving from the improved engine thermal efficiency reduces with ethanol contents. Figure 7 (b) shows the normalised GHG savings. It can be seen that the renewable bioethanol contributes to the majority of the GHG savings, and this dominance is enhanced with ethanol content. Although GHG saving from engine efficiency gain is less than the saving from the use of renewable bioethanol, it comes without additional cost. It should be noted that the values shown in Figure 7 are only for the specific vehicle and ethanol GHG intensity. Values will be changed if different vehicles or ethanol feedstocks are used.

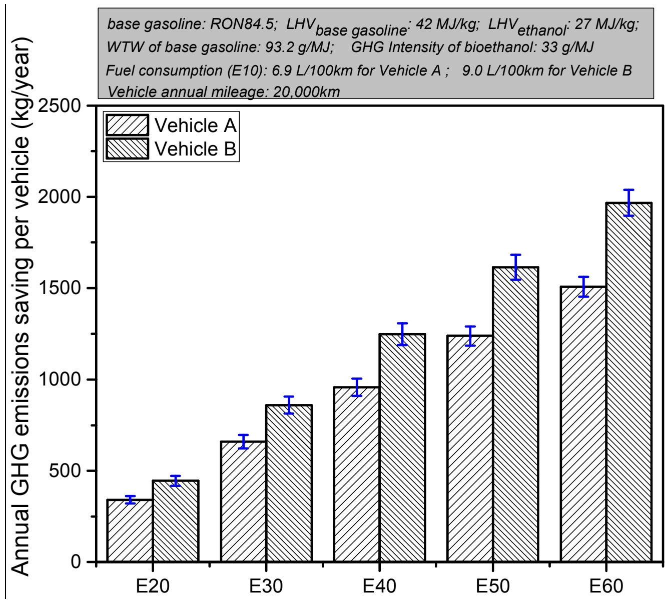

Figure 8: Annual WTW GHG emissions (CO_2 equivalent) for ethanol blends in a TC DISI passenger vehicle

Figure 8 shows the annual WTW GHG savings (CO_2 equivalent) for ethanol blends. It is assumed that the annual vehicle mileage range is 20,000 km. The annual WTW GHG saving is up to 2000 kg in Vehicle B for E60. The saving is linear to ethanol content.

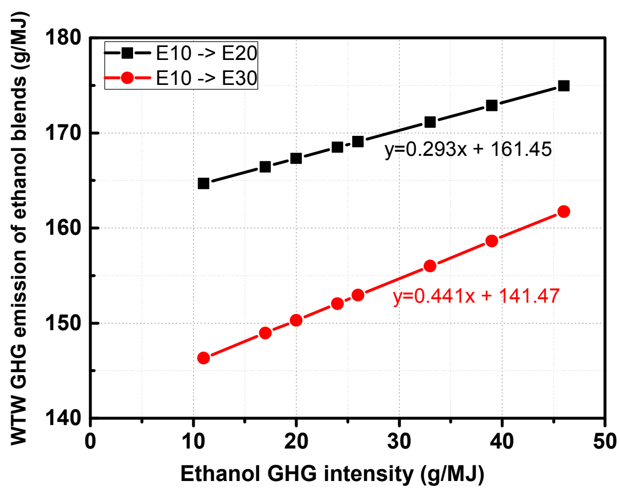

Figure 9: Effect of ethanol GHG intensity on WTW GHG emissions (CO_2 equivalent) of ethanol blends (E20 and E30) in TC DISI vehicles

Figure 9 presents the effect of ethanol GHG intensity on WTW GHG emissions (CO_2 equivalent) of ethanol blends (E20 and E30) in TC DISI vehicles. The ethanol GHG intensity covers the range listed in Table 2. Compared to E10, every 1 $gCO_2\text{-eq/MJ}$ reduction in the bioethanol GHG intensity leads to 0.293 and 0.439 $gCO_2\text{-eq/MJ}$ reduction in the WTW GHG emissions for E20 and E30, respectively. Reducing ethanol GHG intensity is key to reduce WTW GHG emissions of ethanol blends. China heavily relies on coal to generate electricity, and on an average electric vehicle in China produces 259 g/km GHG emission, which is much higher than the values presented in Figure 9. Significant electricity GHG intensity reduction is needed in order to match GHG emissions from an electric car and the vehicle running on ethanol blends. More information about the average electric car GHG emissions per kilometer of various contries can be found in Figure 1A in Appendix.

4 Conclusions

In this paper, an empirical model for spark ignition engines is used to study the engine thermal efficiency gain of ethanol blends using two base gasoline fuels, RON84.5 and RON94.5, typical regular- and premium-octane base gasolines available in China. In addition, using GHG emission data of bioethanol and gasoline in China from the literature, and the engine thermal efficiency gains, this paper presents the estimated WTW GHG savings of ethanol blends. The following are main conclusions drawn from results and discussion:

1. For the ethanol blends with the RON84.5 base gasoline, the reduction of LHV is possibly offset by the gain of thermal efficiency due to the use of high octane ethanol blends. However, for ethanol blends with higher RON base gasoline, it is not possible to offset the reduced LHV; consequently, fuel economy is dramatically reduced with high ethanol blends.
2. Assuming that in China in the future bioethanol has a GHG intensity of 33 gCO_2-eq/MJ, compared to E10, E30 leads to a 21.2% reduction of WTW GHG emissions in a TC DISI vehicle. Among this 21.2% reduction, one third is due to the engine thermal efficiency gain and two third is due to the using of renewable bioethanol.

3. Every 1 gCO_2-eq/MJ reduction in the ethanol GHG intensity leads to 0.293 and 0.439 gCO_2-eq/MJ reduction in the WTW GHG emissions for E20 and E30 in TC DISI vehicles, respectively.

Limitation of this study

This paper does not intend to comment on the benefits of ethanol blends at specific engine operating conditions (load and speed). Instead, it used a model based on historical and literature data to evaluate statistical benefits of ethanol blends on the engine thermal efficiency gains and WTW GHG emissions. The real benefits would be dependent on engine hardware design, and actual vehicle testing cycles. The benefits presented in this paper would be underestimated if engines were operated at knock-limited high load conditions where high-octane ethanol blends are more resistant to knocking than the gasoline base fuel. The benefits would be overestimated if engines were operated at knock-free low load conditions. Also, the engine thermal efficiency gain is estimated to be the same as the reduction of vehicle fuel consumption; this will introduce some errors in the estimation, especially when the engine is downsized. It should be also pointed out that the GHG emissions of ethanol blends mentioned in this paper are estimated based on several assumptions, such as the GHG intensity of bioethanol and engine efficiency gains. Attention should be paid when using those values for further studies.

Appendix

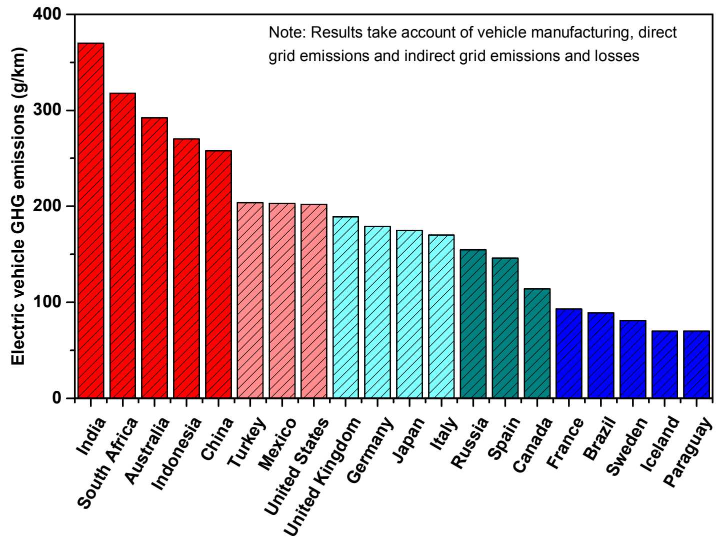

Figure 1A: Electric vehicle GHG emissions (data extracted from Ref.[25], which is originally from DEFRA and IEA et al.[26-28]

Reference

1. Boot, M., Biofuels from Lignocellulosic Biomass: Innovations Beyond Bioethanol. John Wiley & Sons: 2016.

2. Daniel, R.; Wang, C.; Tian, G.; Xu, H.; Richardson, D., Dual-Injection as a Knock Mitigation Strategy using pure Ethanol and Methanol. SAE International 2012-01-1152: 2012.

3. Wang, C.; Xu, H.; Herreros, J. M.; Wang, J.; Cracknell, R., Impact of Fuel and Injection System on PM Emissions from a DISI Engine. Applied Energy 2014, 132, (1), 178-191.

4. Wang, C. M.; Xu, H. M.; Herreros, J. M.; Lattimore, T.; Shuai, S. J., Fuel Effect on Particulate Matter Composition and Soot Oxidation in a Direct-Injection Spark Ignition (DISI) Engine. Energy & Fuels 2014, 28, (3), 2003-2012.

5. Wang, C.; Chahal, J.; Janssen, A.; Cracknell, R.; Xu, H., Investigation of gasoline containing GTL naphtha in a spark ignition engine at full load conditions. Fuel 2017, 194, 436-447.

6. Xu, H.; Wang, C.; Ma, X.; Sarangi, A. K.; Weall, A.; Krueger-Venus, J., Fuel injector deposits in direct-injection spark-ignition engines. Progress in Energy and Combustion Science 2015, 50, (0), 63-80.

7. Caton, P. A.; Hamilton, L. J.; Cowart, J. S., An Experimental and Modeling Investigation into the Comparative Knock and Performance Characteristics of E85, Gasohol [E10] and Regular Unleaded Gasoline [87 (R+M)/2]. SAE International 2007-01-0473: 2007.

8. Kalghatgi, G. T.; Nakata, K.; Mogi, K. Octane appetite studies in direct injection spark ignition (DISI) engines; SAE Technical Paper 2005-01-0244: 2005.

9. Wang, C.; Janssen, A.; Prakash, A.; Cracknell, R.; Xu, H., Splash blended ethanol in a spark ignition engine – Effect of RON, octane sensitivity and charge cooling. Fuel 2017, 196, 21-31.

10. Farrell, J. T.; Weissman, W.; Johnston, R. J.; Nishimura, J.; Ueda, T.; Iwashita, Y., Fuel effects on SIDI efficiency and emissions. SAE transactions 2003, 112, (4), 2394-2412.

11. Miles, P., Fuel/Engine Interactions:Potential for Emissions and Efficiency BenefitsPart1: SI Fuels. Engine Research Center Symposium 2015.

12. Si, S.; Chalfant, J. A.; Cynthia, C.-Y.; Lawell, L.; Yi, F., The effects of China's biofuel policies on agricultural and ethanol markets. Dyson Cornell SC Johnson College of Business: Report 2017.

13. Zhang, T.; Xie, X.; Huang, Z., The policy recommendations on cassava ethanol in China: Analyzed from the perspective of life cycle "2E&W". Resources, Conservation and Recycling 2017, 126, (Supplement C), 12-24.

14. Ren, J.; Tan, S.; Dong, L.; Mazzi, A.; Scipioni, A.; Sovacool, B. K., Determining the life cycle energy efficiency of six biofuel systems in China: A Data Envelopment Analysis. Bioresource Technology 2014, 162, (Supplement C), 1-7.

15. Zhao, L.; Ou, X.; Chang, S., Life-cycle greenhouse gas emission and energy use of bioethanol produced from corn stover in China: Current perspectives and future prospectives. Energy 2016, 115, (Part 1), 303-313.

16. Leng, R.; Wang, C.; Zhang, C.; Dai, D.; Pu, G., Life cycle inventory and energy analysis of cassava-based Fuel ethanol in China. Journal of Cleaner Production 2008, 16, (3), 374-384.

17. Zhang, C.; Han, W.; Jing, X.; Pu, G.; Wang, C., Life cycle economic analysis of fuel ethanol derived from cassava in southwest China. Renewable and Sustainable Energy Reviews 2003, 7, (4), 353-366.

18. Yang, Q.; Chen, G., Greenhouse gas emissions of corn–ethanol production in China. Ecological modelling 2013, 252, 176-184.

19. Wang, C.; Zeraati-Rezaei, S.; Xiang, L.; Xu, H., Ethanol blends in spark ignition engines: RON, octane-added value, cooling effect, compression ratio, and potential engine efficiency gain. Applied Energy 2017, 191, 603-619.
20. Mittal, V.; Heywood, J. B., The shift in relevance of fuel RON and MON to knock onset in modern SI engines over the last 70 years. SAE International Journal of Engines 2009, 2, (2009-01-2622), 1-10.
21. Leone, T. G.; Anderson, J. E.; Davis, R. S.; Iqbal, A.; Reese, R. A.; Shelby, M. H.; Studzinski, W. M., The Effect of Compression Ratio, Fuel Octane Rating, and Ethanol Content on Spark-Ignition Engine Efficiency. Environmental science & technology 2015, 49, (18), 10778-10789.
22. 康利平; Dror, M. B.; 秦兰芝; 安峰, Innovation Center for Energy and Transportation: 中国乘用车燃料消耗量发展年度报告 2016. 2016.
23. EC, Directive 2009/28/EC of the European Parliament and of the Council of 23 April 2009 on the promotion of the use of energy from renewable sources and amending and subsequently repealing Directives 2001/77/EC and 2003/30/EC. Official Journal of the European Union 2009, (L 140/16).
24. Li, X.; Ou, X.; Zhang, X.; Zhang, Q.; Zhang, X., Life-cycle fossil energy consumption and greenhouse gas emission intensity of dominant secondary energy pathways of China in 2010. Energy 2013, 50, (Supplement C), 15-23.
25. Wilson, L., Electric car's carbon emissions around the globe. 2013.
26. DEFRA, 2012 Guidelines to Defra / DECC's GHG Conversion Factors for Company Reporting. 2012.
27. Hawkins, T. R.; Singh, B.; Majeau-Bettez, G.; Strømman, A. H., Comparative environmental life cycle assessment of conventional and electric vehicles. Journal of Industrial Ecology 2013, 17, (1), 53-64.
28. IEA, CO2 Emissions from Fuel Combustion. 2012.